Indian J Phys. 80 (12), 1179-1187 (2006)

Study of electromagnetic ion-cyclotron wave with general loss-cone distribution function

G Ahirwar, P Varma and M S Tiwari*

Department of Physics and Electronics,
Dr H S Gour University,
Sagar – 470 003 Madhya Pradesh, India

E-mail tiwarims@rediffmail.com

Received 30 March, 2006, accepted 20 November 2006

Abstract Electromagnetic ion-cyclotron (EMIC) waves have been studied by single particle approach with general loss-cone distribution function. The dispersion relation, growth rate, resonance energy and marginal stability of the electromagnetic ion-cyclotron wave with general loss-cone distribution function in a low β homogeneous plasma have been investigated. The effect of the steepness of the loss-cone distribution has been studied with different plasma parameters. The wave is assumed to propagate parallel to the static magnetic field. The whole plasma is considered to consist of resonant and non-resonant particles. It is assumed that resonant particles participate in energy exchange with the wave whereas non-resonant particles participate in the oscillatory motion of the wave. The effect of general loss-cone distribution function is to enhance the growth rate of EMIC waves. The results are interpreted for the space plasma parameters appropriate to the auroral acceleration region of the earth's magnetoplasma.

Keywords Cyclotron wave, electromagnetic ion-cyclotron instability, auroral acceleration region, solar plasma, loss-cone distribution function

PACS Nos. 52.35.Hr, 52.35.Qz, 94.10.Rk

1. Introduction

The geomagnetic micro-pulsations in the frequency range 0.1-5 Hz have been explained by various workers in terms of ion cyclotron instability arising due to the interaction of streaming protons and the left-hand circularly polarized electromagnetic wave. The emission occurs at frequencies corresponding to ion cyclotron instability. Cornwall *et al* [1] suggested that if the ring current protons penetrated the plasma-pause, intense resonant electromagnetic ion-cyclotron turbulence would lead to their loss by precipitation.

Experimental evidence for naturally occurring ion cyclotron instability has been summarized by Cornwall [2]. It has been clearly pointed out that both particle precipitation and wave generation are observed to occur preferentially in the regions of high density of cold electrons. Cornwall and Schulz [3] discussed the electromagnetic ion cyclotron instability in the presence of cold plasma and gave analytical expressions for the growth rates as a function of wave frequency ω. They also concluded that this instability becomes important when the densities of cold and hot plasma are comparable. Ion-cyclotron electromagnetic instability in the presence of warm and cold plasma was studied in details by Cuperman and Gomberoff [4].

Cuperman and Gomberoff [4] have stated that a number of authors have pointed out that the generation of electromagnetic ion-cyclotron (EMIC) waves would pitch-angle scatters protons, subsequently reducing their fluxes. Plasma sheet protons are injected into the magnetosphere during magnetic storm. Radial diffusion then transports these protons across the plasma-pause where they destabilize electromagnetic ion-cyclotron waves [4]. When the proton flux inside the plasma is large enough, there is rapid EMIC wave growth. Some protons are then forces into the loss-cone and are precipitated with a lifetime of the order of one hour. In the recovery phase of the storm, the plasmapause moves out of $1 \sim 6\ R_E$ (R_E is the earth's radius) and the plasma-sphere is filled by ambipolar diffusion of cold ionospheric plasma [4]. Thus, the higher density plasma causing EMIC wave generation and proton precipitation envelops the stably trapped outer ring current protons. Theoretical investigations of the EMIC

*Corresponding Author

instability for plasma parameters of magnetospheric interest have been carried out by many workers [4-6] Observationally, the detection of up to 30 Hz magnetic fluctuations with amplitudes about 10^{-5} G near the plasmapause and in the proton ring current during initial, main and recovery phase is consistent with the assumption of EMIC waves [4]

In past Jordanova *et al* [5] have stated that ring current ion distribution are often unstable and can generate different classes of plasma waves in the equatorial magnetosphere like magnetosonic, electromagnetic ion cyclotron (EMIC) waves *etc* The subsequent interaction occurs with an energetic particle and a plasma wave in pitch angle scattering and energy exchange between the particle and the wave [5] Scattering of ring current particles into the loss cone due to resonant interactions with EMIC waves occurs on short timescales and could contribute significantly to ion loss [1,5,7], especially during the main phase of the storm when ring current energy loss timescales may be as low as 5 – 1 hours [8] The plasma waves can also transfer energy from ring current H^+ to O^+ during magnetic storms [5, 9,10] and play an important role in the heating of the thermal electrons and ions [5,11-14]

The observational evidences of EMIC waves have been provided by Jordanova *et al* [5] as ion electron waves were observed by the magnetic field experiment on board ATS 6, [15] and on board GEOS 1 and 2, [16] The authors in both the studies found that left-hand polarized EMIC waves predominantly occurred in the dusk bulge region, in association with increasing thermal H_e^+ populations and anisotropic pitch angle distributions of ring current ions of energies greater than 20 keV [5] Observations by the Active Magnetospheric Particle Tracer Explorers / CCE (AMPTE / CCE) spacecraft showed maximum occurence (10-20 %) of EMIC (Pc1) waves with left –hand polarization near the equator between 1000 and 1800 magnetic local time (MLT) at large L>7, [5,17] At L<5, waves occurred with smaller probability (<1%) and had a relatively uniform local time variation A statistical study of Pc1 waves measured at ionospheric altitudes by the DE 2 satellite was performed by Erlandson and Anderson [5,18] Most of the events were observed in the dawn (0400-0600 MLT) and noon (1000-1500 MLT) sectors from 50° to 62° invariant latitude (INV). However, it was noted that detection of waves at high latitudes (INV > 65°) was limited by noise effects [5] The ionospheric Pc1 occurrence rate of 1-2 % at L=3-5 was slightly larger than the Pc1 occurrence rate in the equatorial magnetosphere at L<5, [5,17] and might to be due to differences in the properties of the dawn and noon sector events The authors concluded that the source of noon sector ionospheric Pc1 waves is EMIC waves generated in the equatorial magnetosphere, while the source of the dawn sector waves is less certain [5]

The acceleration of ions perpendicular to the ambient magnetic field at the auroral latitudes has been extensively reported by various workers [19]. A large number of observational evidences are available to predict transverse ion acceleration and ion conic formation at the auroral latitudes [19-21] A statistical study of electromagnetic ion-cyclotron emissions in association with the ion-conics and field aligned electrons occurring within inverted – V structures has been presented by Lund *et al* [19] They have described that when EMIC waves accompany an ion conics H_e^+ is found to be energized more efficiently than other species [22] and O^+ is preferentially accelerated over H^+ [23,24] The H_e^+ ions are apparently accelerated by a cyclotron resonant interaction with the waves near the altitude where their frequency equals the helium gyro frequency f_{cHe} Their statistical study described shows, almost all of the ion conic events seen by FAST are associated with either BBELF emissions or EMIC waves

The distribution of EMIC ion conics over MLT and invariant latitudes is similar to that of ion beams [19,25,26] In fact ion beams frequently occur at one or both edges of an EMIC ion conic This association leads us to speculate that the change in altitude of the bottom of the potential drop with horizontal position may play a role in generating the EMIC waves, this conjecture could resolve the discrepancy noted by Lund and LaBelle [27] that the growth rates of the traditionally assumed beam generation mechanism [28] are too low to account for the observed waves [19]

In this paper we present a systematic and detail investigation of EMIC instabilities with loss-cone distribution function for magnetosphere like plasma parameters with the purpose of attaining a more complete understanding of their relative importance In most of the theoretical work reported so far, the velocity distribution function has been assumed to be either Maxwellian or bi-Maxwellian ignoring the steep loss feature. Plasma in mirror like devices and in the auroral region with curved and converging magnetic field lines, considered depart from Maxwellian distribution and have steep loss-cone distribution, [29-31] provided there is relatively low degree of plasma collisionality

Effects of the general distribution function have been widely studied by number of workers on the electrostatic waves electromagnetic waves, drift waves, Alfven and kinetic Alfve waves, ion cyclotron waves, electrostatic ion cyclotron wave [29,30,32,33] In this paper the general distribution function is used to study EMIC waves

The basic trajectory is evaluated in section 2 Section describes the evaluation of perturbed densities. The dispersion relation is evaluated in section 4. In section 5 we have evaluated the wave energy with growth rate of the wave. Section 6 deals with the marginal instability Section 7 deals with the result and discussions.

2. Basic Trajectories

The wave propagating in the direction of the ambient magnetic field along the z-axis is considered. The whole plasma has been considered to consist of resonant and non-resonant particles. The resonant particles participate in energy exchange with the waves, whereas the non-resonant particles support the oscillatory motion of the wave. The particles having their parallel velocities equal to the phase velocity of the wave are defined as resonant particles, otherwise non-resonant. The EMIC wave is assumed to start at $t = 0$ when the resonant particles are not yet disturbed. The trajectories of the particles are evaluated with the framework of linear theory. Taking the particle trajectory in the presence of EMIC wave the dispersion relation, energy calculation and growth rate is derived for different distribution indices.

The left-handed circularly polarized EMIC wave having angular frequency ω is defined as [31],

$$B_x = B\cos(kz - \omega t)$$

$$B_y = B\sin(kz - \omega t) \tag{1}$$

When the system is co-moving with the wave, the electric field vanishes. Thus the wave magnetic field has the form,

$$B = B_x[\cos kz]\,x + B_y[\sin kz]\,y \tag{2}$$

where the following conditions are valid,

$$z^{wave} = z^{lab} - (\omega/k)\,t \tag{3a}$$

$$v^{wave} = v^{lab} - (\omega/k) \tag{3b}$$

Since $ck/\omega >> 1$, the magnetic field amplitude may be regarded in both system identical. Thus the equation of ion motion in the wave is given as

$$\frac{dv}{dt} = \frac{q}{mc}\left[(v \times B_0) + (v \times B)\right] \tag{4}$$

We take the cylindrical variables in velocity space as

$$v_x = V_\perp \cos\phi$$

$$v_y = V_\perp \sin\phi \tag{5}$$

$$v_z = V_{II}$$

Then the equation of motion is written as [31]

$$\frac{dV_\perp}{dt} = -hV_{II}\Omega\sin(kz - \phi) \tag{6}$$

$$\frac{dV_{II}}{dt} = -hV_\perp\Omega\sin(kz - \phi)$$

Where $h = B/B_0$ is the ratio of electromagnetic to static magnetic field amplitude and $\Omega = qB_0/mc$ is the ion cyclotron frequency. When the amplitude of electromagnetic wave is smaller as compared to static magnetic field, we apply $h<<1$ to evaluate the approximate particle trajectory for resonant and non-resonant particles by perturbation theory [31]. Consider the expansion of the form

$$V_\perp = V_{\perp 0} + \delta V_\perp \tag{7}$$

$$V_{II} = V_{II0} + \delta V_{II}$$

Where $V_{\perp 0}$, V_{II0} are the initial values at $t = 0$. Substituting eq (6) in (7) we find the following set of equations [31]

$$\delta V_\perp = \left[h\Omega(V_{II0} - \omega/k)\right]/\left[kV_{II0} - (\omega - \Omega)\right]\left[\cos(kz - \omega t - \psi) - \varepsilon\cos\left(kz - \omega t - \psi - (kV_{II0} - (\omega - \Omega))t\right)\right]$$

$$\delta V_{II} = -hV_{\perp 0}\Omega/\left[kV_{II0} - (\omega - \Omega)\right]\left[\cos(kz - \omega t - \psi) - \varepsilon\cos\left(kz - \omega t - \psi - (kV_{II0} - (\omega - \Omega))t\right)\right] \tag{8}$$

where $z = z_0 + V_{II}t$ and $\psi = \psi_0 - \omega t$ and $\varepsilon = 0, 1$ for the non-resonant and resonant particles.

3. Density Variation

To determine the dispersion relation and the growth-rate, we consider a bi-Maxwellian plasma with density distribution as

$$N(v, \bar{V}) = N_0 f_\perp(V_\perp) f_{II}(V_{II}) \tag{9}$$

We consider a general distribution function for $f_\perp(V_\perp)$ as [31,34-36]

$$f_\perp(V_\perp) = \left[V_\perp^{2J}/\left(\pi V_{T\perp}^{2(J+1)} J!\right)\right]\exp\left(-V_\perp^2/V_{T\perp}^2\right) \tag{10}$$

and $f_{II}(V_{II})$ which is defined by the drifting Maxwellian [35]

$$f_{II}(V_{II}) = \left(1/\sqrt{\pi}V_{TII}\right)\exp\left(-V_{II}^2/V_{TII}^2\right) \tag{11}$$

where J is the distribution index and measures the steepness of the loss-cone feature [29,34,35]. In the case of $J = 0$ this represents a bi-Maxwellian distribution and for $J = \infty$ this reduces to the Dirac delta function [29]. $V_{TII}^2 = 2T_{II}/m$ and $V_{T\perp}^2 = (J+1)^{-1}2T_\perp/m$ are the squares of parallel and perpendicular thermal velocities with respect to the external magnetic field.

We evaluate the density perturbation associated with the particle velocity [31] as

$$dn_1/dt = -N(V)(\nabla\, u) \tag{12}$$

Transforming the r.h.s of eq. (12) as the function of t and by equation (8) and (12) we get the solution for perturbed density [31] as,

$$n_1 = \left(hV_{\perp 0}\Omega kN(V)\right)\Big/\left[kV_{\Pi 0} - (\omega - \Omega)\right]^2$$

$$\left[\cos\chi - \varepsilon\cos\chi_0 + \varepsilon t\,\Lambda\sin(\chi - \Lambda t)\right] \tag{13}$$

where $\chi = kz - \omega t - \psi$ and $\Lambda = \left(kV_{\parallel 0} - (\omega - \Omega)\right)$

4. Dispersion relation

The existence of the ion energy anisotropy has been established and the growth is possible only when $T_\perp/T_{II} > 1$ Thus we are interested in the behavior of those particles for which $T_\perp/T_{II} > 1$. Then we consider the cold plasma dispersion relation for the EMIC wave [37] as

$$c^2k^2/\omega^2 = \left(\omega_{pi}^2/\Omega^2\right)(1 - \omega/\Omega)^{-1} \tag{14}$$

where $\omega_{pi}^2 = 4\pi N_0 e^2/m_{i,e}$ is the plasma frequency for the ions We have adopted the cold plasma dispersion relation for the electromagnetic ion-cyclotron wave as derived in past by Kennel and Petscheck [37] Since the effect of loss-cone appears through the temperature anisotropy [38], thus the cold plasma dispersion relation equation (14) is not affected by loss-cone indices

5. Wave energy and growth rate

The wave energy density W_w per unit wavelength is the sum of the pure field energy and the changes in the energy of the non-resonant particles *i.e.* the total energy per unit wavelength is given as

$$W_w = U + W_i. \tag{15}$$

Where U is the energy of electromagnetic wave as defined by the expression [31] as,

$$U = (1/16\pi)\left[(d/d\omega)(\omega\varepsilon_{ik})\,E_1^* E_k + |B|^2\right] \tag{16}$$

Where ε_{ik} is the dielectric tensor. After the calculation, the electromagnetic wave energy per unit wavelength is given by

$$U = \left(\lambda B^2/8\pi\right)\left[(2\Omega - \omega)/(\Omega - \omega)\right] \tag{17}$$

and
$$W_i = \int_0^\lambda dz \int_0^{2\pi} d\psi \int_0^\infty V_\perp dV_\perp P \int_{-\infty}^{\infty} dV_\Pi\, m/2 \times \left[(N + n_1)(V + \delta V)^2 - NV^2\right] \tag{18}$$

5.1 Non-resonant energy

With the help of eq (8), (13) and (18) with $\varepsilon = 0$ we find the parallel non resonant energy as [31]

$$W_{i\Pi} = -\lambda B^2/8\pi\; C_J/V_{T\Pi}^2\,\omega_{pi}^2/c^2k_\Pi^2\left[1/2Z_1(\zeta) + (\omega - \Omega)\Big/\left(k_\Pi V_{T\Pi}\right)Z_2(\zeta)\right] \tag{19}$$

and perpendicular non-resonant energy as

$$W_{i\perp} = \lambda/2\; B^2/8\pi\,\omega_{pi}^2/c^2k_\Pi^2\left[D_J\left(1 - (2\Omega/k_\Pi V_{T\Pi})Z(\zeta) + \left(\Omega^2/k_{II}^2V_{T\Pi}^2\right)Z_1(\zeta)\right) + \left(2C_J/V_{T\Pi}^2\right)\left(Z_1(\zeta) - (\Omega/k_\Pi V_{T\Pi})Z_2(\zeta)\right)\right] \tag{20}$$

5.2 Perpendicular Resonant energy

The perpendicular (transverse) energy and the parallel resonant energy of the resonant ions are calculated with the help of eq (8), (13) and (18) with $\varepsilon = 1$ as [31]

$$W_{r\perp} = \lambda/4\left(B^2\omega_{pi}^2/C^2k_\Pi^2\right)t\left[C_J + \left(2\Omega^2/k_{II}^2\right)D_J\right]f_i(V_r) - C_J(\Omega/k_\Pi)f'(V_r)$$

$$W_{r\perp} = \left(\pi^{1/2}B^2\omega_{pi}^2/C^2k_\Pi^2\right)\times\left(\Omega_i^2/\omega\; k_\Pi^2V_{III}\right)\left[C_J/V_{TII}^2(\omega - \Omega_i/\Omega_i) + D_J + 1/2\left(k^2/\Omega^2\right)C_J\right]\exp\left[-\left((\omega - \Omega_i)^2/k_\Pi^2V_{III}^2\right)\right] \tag{22}$$

and
$$W_{r\perp} = \left(\pi^{1/2}B^2\omega_{pi}^2/C^2k_\Pi^2\right)\times\left(\Omega_i^2/\omega\; k_\Pi^2V_{T\Pi}\right)\left[(J+1)T_\perp/T_\Pi\left((\omega - \Omega_i)/\Omega_i\right) + 1\right]\exp\left[-(\omega - \Omega_i)^2/k_\Pi^2V_{T\Pi}^2\right. \tag{23}$$

5.3 Parallel Resonant energy

$$W_{r\Pi} = -\lambda/4\left(B^2\omega_{pi}^2/c^2k_\Pi^2\right)tC_J\left((\omega - \Omega)/k_\Pi - V_\Pi\right)f'(V_r$$

$$W_{r\Pi} = \left(\pi^{1/2}B^2\omega_{pi}^2/C^2k_\Pi^2\right)\times\left(\Omega_i^2/\omega\; k_\Pi^2V_{T\Pi}\right)\left[\left(C_J/V_{T\Pi}^2\right)(\omega - \Omega_i/\Omega_i)^2\right]\exp\left[-(\omega - \Omega_i)^2/k_\Pi^2V_{TII}^2\right] \tag{25}$$

$$W_{r\Pi} = \left(\pi^{3/2}B^2\omega_{pi}^2/C^2k_\Pi^2\right)\times\left(\Omega_i^2/\omega\; k_\Pi^2V_{TI}\right)\left[(J+1)T_\perp/T_\Pi\left((\omega - \Omega_i)/\Omega_i\right)^2\right]\exp\left[-(\omega - \Omega_i)^2/k_\Pi^2V_{TII}^2\right. \tag{26}$$

here

$$C_J = \left(2\pi/V_{T\perp}^{2(J+1)}\, J!\right)\int_0^{\infty} dV_\perp^2 V_\perp^{2(J+1)} \exp\left(-V_\perp^2/V_{T\perp}^2\right)$$

$$D_J = \left(2\pi/V_{T\perp}^{2(J+1)}\, J!\right)\int_0^{\infty} dV_\perp^2 V_\perp^{2J} \exp\left(-V_\perp^2/V_{T\perp}^2\right)$$

$$f_r(V_r) = \left(m/2\pi T_{\Pi_i}\right)^{1/2} \exp\left[-m(\omega-\Omega)^2/2T_{\Pi_i}k_\Pi^2\right]$$

$$f'(V_r) = -2\left(m/2\pi T_{\Pi_i}\right)^{1/2}\left(\omega-\Omega/k_\Pi V_{T\Pi_i}^2\right) \exp\left[-\left(\omega-\Omega/k_\Pi V_{T\Pi_i}\right)^2\right]$$

$$Z_n(\xi - V_D/V_{T\Pi}) = 1/\sqrt{\pi}\; p\int\left(\exp(x^2)/(x-\xi)^{n+1}\right)dx$$

$$\xi = (\omega-\Omega)/k_\Pi V_{\Pi\Pi}$$

Using the law of conservation of energy

$$d/dt\,(W_r + W_w) = 0 \tag{27}$$

The growth / damping rate γ is derived as [31]

$$\partial U/\partial t = 2\gamma U \tag{28}$$

where

$$dW_r/dt = -2\,\partial U/\partial t$$

and

$$dW_i/dt \sim \partial U/\partial t$$

Those particles with velocities near the phase velocity of the waves give up an energy 2U to the waves. Half of this goes to potential energy and the other half goes into kinetic energy of oscillation of the bulk of the particles. Hence the growth rate is obtained as

$$\frac{\gamma}{\omega} = \frac{\dfrac{\Omega}{kV_{\Pi}}\left[\dfrac{(\Omega-\omega)}{\Omega}\dfrac{(J+1)V_{T\perp}^2}{V_{T\Pi}^2} - 1\right]\exp\left[-\dfrac{1}{V_{T\Pi}^2}\left(\dfrac{\omega-\Omega}{k_{\Pi}}\right)^2\right]}{\left(\dfrac{ck}{\omega_{pi}}\right)^2\left(\dfrac{2\Omega-\omega}{\Omega-\omega}\right)+\dfrac{1}{2}\dfrac{\omega^2}{(\Omega-\omega)^2}} \tag{29}$$

Using the value of $V_{T\perp}^2 = (J+1)^{-1}(2T_\perp/m)$ and $V_{T\Pi}^2 = 2T_{\Pi}/m$

$$\frac{\gamma}{\omega} = \frac{\dfrac{\Omega}{kV_{\Pi}}\left[\dfrac{(\Omega-\omega)}{\Omega}\dfrac{(J+1)T_\perp}{T_{\Pi}} - 1\right]\exp\left[-\dfrac{1}{V_{T\Pi}^2}\left(\dfrac{\omega-\Omega}{k_{\Pi}}\right)^2\right]}{\left(\dfrac{ck}{\omega_{pi}}\right)^2\left(\dfrac{2\Omega-\omega}{\Omega-\omega}\right)+\dfrac{1}{2}\dfrac{\omega^2}{(\Omega-\omega)^2}} \tag{30}$$

Here it is noticed that J has affected the growth rate through the temperature anisotropy as discussed by Summers and Thorne, [38] for the electromagnetic waves propagating parallel to the magnetic field with general loss-cone distribution function

6. Marginal instability

For the marginal instability condition $\gamma = 0$, the maximum stable frequency is obtained

$$\omega = \Omega\left(1 - 1/(J+1)\; T_{\Pi}/T_\perp\right) \tag{31}$$

The equation (31) is derived by imposing the condition of $\gamma/\omega = 0$ as the marginal instability condition in equation (30)

7. Result and discussions

For the numerical evaluation of the dispersion relation, resonant energies and growth rate with the steepness of loss-cone distribution, the following plasma parameter are used which are relevant for the auroral acceleration region [39,40]

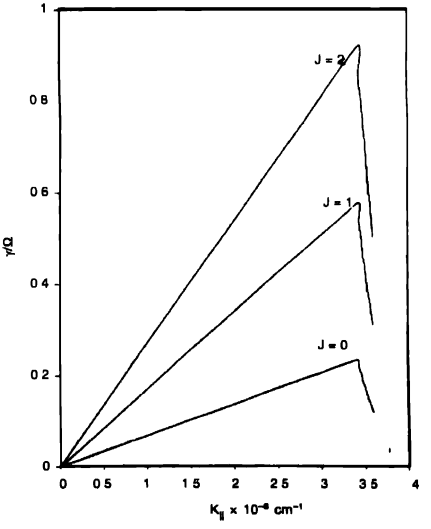

Figure 1. Variation of growth rate (γ/Ω_i) *versus* wave vector k_{Π} cm^{-1} for different values of distribution indices J and $T_\perp/T_{\Pi}$ =80

$B_0 = 4300\,\text{nT}, R_E = 1.4 \cdot 2,\ \Omega_i = 412\,\text{s}^{-1},$

$V_{T\|i} = 6.41 \times 10^8\,\text{cm/sec} \quad \omega_{pi}^2 = 1.732 \times 10^6\ \text{sec}^{-2}$

Figure 1 shows the variation of growth rate γ/Ω with wave vector ($k_\|$) for different values of distribution indices J at the fixed value of $T_\perp/T_\| = 80$. It is observed that the higher distribution indices enhance the growth rate. Thus the mirror like structure of the magnetosphere with a steep loss-cone may depart from Maxwellian with unstable EMIC wave emissions. At higher $k_\|$ the wave growth has enhanced according to increase of J, which may be due to the wave particle interaction.

Figure 2 shows the variation of transverse (perpendicular) resonant energy $W_{r\perp}$ *versus* wave vector $k_\|$ for different values of distribution indices J at $T_\perp/T_\| = 80$. The effect of increasing distribution index is to decrease the perpendicular resonant energy for the particular value of $k_\|$. However, higher values of $k_\|$ are needed to enhance $W_{r\perp}$ at higher J values. Thus the steepness of the loss-cone distribution of the magnetosphere stabilizes the transverse energy at the perpendicular $k_\|$. It is also observed that $W_{r\perp}$ increases with the increasing values of $k_\|$, which implies that perpendicular heating of ions as well as wave emission at particular value of $k_\|$ at which the growth rate is maximum.

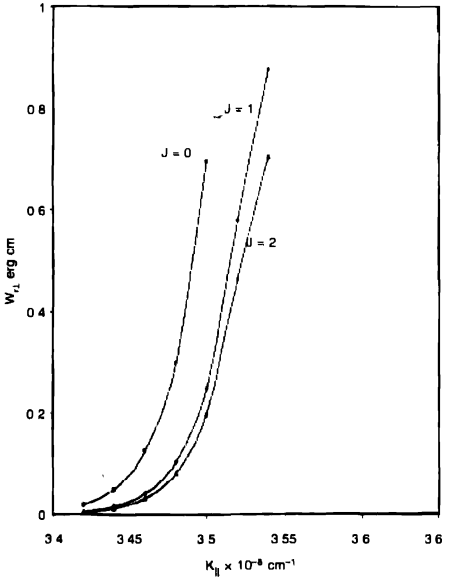

Figure 2 Variation of perpendicular resonant energy $W_{r\perp}$ erg cm *versus* wave vector $k_\|$ cm^{-1} for different values of distribution indices J and $T_\perp/$

ISEE 1 and 2 observations have been made of numerou bursts of polarized transverse EMIC waves in the 50-500 mH frequency range in the near Earth's magnetotail. Transversel accelerated ions cause strong heating preferentially in th presence of EMIC waves owing to the acceleration in thei cyclotron motion. The total energy of the ions rapidly increase and they become subject to the ∇B or mirror force by means o which they are ejected for the perpendicular energization. Th frequency of transversely accelerated ions indicated th transverse acceleration of ionospheric ions is a usual an normal process in the high latitude ionosphere ongoing at al times over a wide area approximately coincident with the aurora oval. In past transversely accelerated ions and their associatio with EMIC have been reported by the analysis of FAS observations [19]. The steep loss-cone controls the heatin rate of the transversely accelerated ions through the EMI instability in the auroral acceleration region. The transvers acceleration of the ions may be due to the damping of the EMI waves also.

Figure 3 shows the variation of parallel resonant energy $W_{r\|}$ with wave vector $k_\|$ for different values of distribution indices at $T_\perp/T_\| = 80$. Here it is observed that the effect of increasin values of distribution index J is to increase the parallel resonan energy for particular $k_\|$. Thus the steep loss-cone distributio of the magnetosphere enhances the parallel resonant energy b the EMIC waves. The enhancement of $W_{r\|}$ due to the stee loss-cone by different instabilities has also been reported b

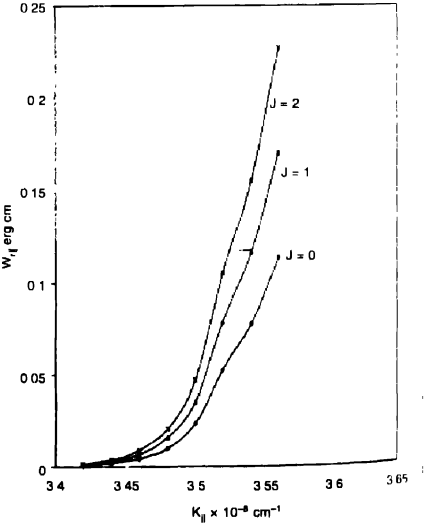

Figure 3 Variation of parallel resonant energy $W_{r\|}$ erg cm vector $k_\|$ cm^{-1} for different values of distribution indices J and $T_\perp/T_\| =$

various workers [30,36] The steep loss-cone structure is analogous to mirror like devices with higher mirror ratio, which may accelerate the charged particles moving along the magnetic field [32,41]. Thus the ion acceleration along the magnetic field is predicted by EMIC wave along the auroral field lines These figures also depict that maximum energy transfer occur at the wave number where EMIC wave has the enhanced growth rate. The energy transfer perpendicular and parallel to the magnetic field are apposite to each other by steep loss-cone effect

Figure 4 shows the variation of growth rate γ/Ω with wave frequency ω/Ω for different values of temperature anisotropies $T_\perp/T_{||}$ at $J = 0$, 1, and 2 respectively It is seen that the growth rate of EMIC wave is positively enhanced with temperature anisotropy $T_\perp/T_{||}$ according to the increase of distribution function J Thus the steep loss-cone distribution of the magnetosphere may be unstable for the wave emissions at lower $T_\perp/T_{||}$ also as depicted in figures The increasing values of $T_\perp/T_{||}$ is to increase the growth rate of the EMIC wave at particular J

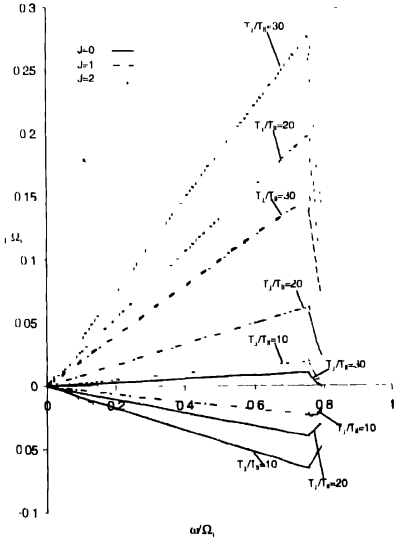

Figure 4 Variation of growth rate γ/Ω_i *versus* wave frequency (ω/Ω_i) at different values of temperature anisotropies $T_\perp/T_{||}$ at different distribution indices J

The energy for the magnetospheric EMIC waves comes from the anisotropic energetic (10 to few 100 keV, *i.e.* ring current and plasma sheet type) protons for which $T_\perp/T_{||} > 1$ Energy can be transferred between the particles and the waves when the particle gyro-frequency matches the Doppler shifted wave frequency The effective amplification of EMIC waves depends on the amount of time spent propagating through a finite growth region [42] Since the magnetic field lines have minimum field strength at the equator, where also the energetic ion fluxes and anisotropies peak, the wave growth may occur there. The EMIC waves generated inside the magnetosphere are in the 0 1-5 H_z frequency range, and are called P_c 1-2 pulsation and ULF waves when seen on the ground

Figure 5 depicts the variation of transverse resonant energies $W_{r\perp}$ with wave frequency ω/Ω for different values of temperature anisotropie $T_\perp/T_{||}$ at $J = 0$, 1, and 2 respectively The effect of increasing values of distribution indices is to decrease the resonant transverse energy as seen in figures Thus the steep loss-cone distribution of the magnetosphere extracts the transverse energy as the wave frequency approaches the cyclotron frequency It is also seen that the $W_{r\perp}$ decreases with the increasing values of ω/Ω which implies that energy is transferred from the particles to the wave

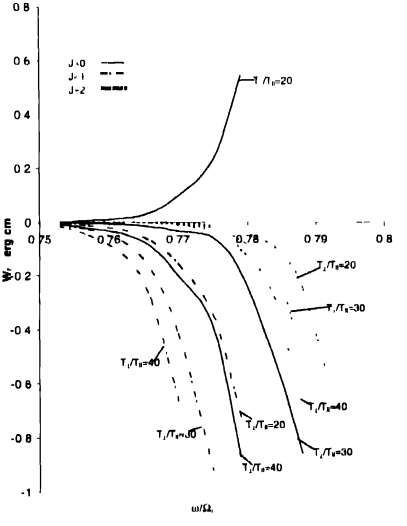

Figure 5 Variation of perpendicular resonant energy $W_{r\perp}$ erg cm *versus* wave frequency (ω/Ω_i) for different values of temperature anisotropies $T_\perp/T_{||}$ at different distribution indices J

Figure 6 shows the variation of parallel resonant energy $W_{r||}$ with wave frequency ω/Ω for different values of temperature anisotropies $T_\perp/T_{||}$ at $J = 0$, 1, and 2 respectively Here it is noticed that the effect of increasing values of distribution indices is to decrease the parallel resonant energy with increase of $T_\perp/T_{||}$. Thus the steep loss-cone distribution of the magnetosphere stabilizes the parallel resonant energy of EMIC

waves according to the frequency of wave The effect become maximum as wave frequency approaches the cyclotron frequency at higher J values Thus steep cone distribution enhances the wave emission of EMIC mode as well as controls the heating of the ions parallel and perpendicular to the magnetic field The mirroring force may become operative in association with EMIC wave to control the heating and to emit the wave

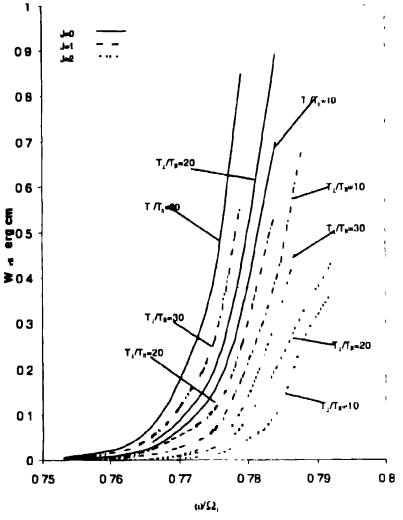

Figure 6. Variation of parallel resonant energy $W_{\parallel}$ erg cm versus wave frequency (ω/Ω_i) for different values of temperature anisotropies $T_{\perp}/T_{\parallel}$ at different distribution indices J

In past various workers by the analysis of low altitude satellite data and on the basis of comparison with ground observations of P_c 1 pulsation a type of energetic proton precipitation closely related to generation of electromagnetic ion-cyclotron (EMIC) waves was found and described [1] It is localized (~ 1 in latitude) precipitation burst within the zone of highly anisotropic fluxes equatorward the isotropy boundary Theoretical predictions on generation the EMIC waves (P_c 1 pulsations) in the near-Earth equatorial plane region, where drifting energetic proton contact the cold plasmaspheric plasma, experimentally confirmed using complex observations of cold plasma, hot particles and waves onboard several high and low-orbiting satellites. The EMIC wave generation occurs within localizes tubes with enhanced cold plasma density The observations suggested multiple sources of the waves and related proton precipitation (Brief report by Polar Geophysical Institute (PGI) during 1999-2002 by Dr E. D Tereschenko)

The FAST satellite has detected a class of ions conic events in which H_e^+ is more strongly accelerated than H^+ or O^+ [46] The helium ions in these events typically have 3-30 times the energy of simultaneously observed protons, unlike most conics, in which no strong preferential acceleration occurs [46] These events are well correlated with the occurrence of electromagnetic ion-cyclotron (EMIC) waves and are associated with inverted -V electron distribution [46] Transverse acceleration of ions, which leads to the formation of ion conics, is a ubiquitous feature of the aurora Although lower hybrid waves and ULF waves have been suggested as candidates for heating ions [46] The heating is much more efficient when part of the wave energy is transferred at the ion cyclotron frequency since the waves and particles can then interact resonantly [43,46] Three types of wave emissions are associated with ion conics in the aurora [21] The most common is broad band extremely low frequency (BBELF) emission, but electromagnetic ion-cyclotron (EMIC) waves are found in a sizeable number of cases, particularly in the pre midnight [22,44,46]

Pitch angle diffusion of ring current protons is one of the commonly postulated mechanism employed to explain ring current losses during the magnetic storm recovery phase [45] It is considered that the wave particle interaction with EMIC waves scatters particles into the loss-cone, which was shown by results through the comparative study of distribution function as well as the temperature anisotropy [45]. The role of EMIC is therefore important in determining the time constants of magnetospheric processes and associated energy losses EMIC waves have been observed over many years on the ground as P_c 1,2 waves such as pearl pulsations and intervals of pulsations with diminishing period (IPDP) [45] These studies have provided the bouncing wave packet propagation model However it is only over the last decade that meaningful satellite observations undertaken geo-stationary orbit and GTO and similar elliptical orbits have become available [45]

The study of EMIC waves employed to explain various phenomena related to space plasma as well as laboratory plasma The equilibrium dipolar magnetic field of the earth is curved in the meridional plane and may introduce loss-cone effects in the particle distribution function. Thus the behavior studied for the EMIC wave may be of importance in the electromagnetic emis in the auroral acceleration region [19] In most of the theoretical work the velocity distribution functions have been assumed to be ideal Maxwellian ignoring the loss-cone feature, although most turbulent heating experiments have been done in mirror like devices, which in general allow non-Maxwellian particularly loss-cone distribution The theory developed in the present work may be applicable to such hot particle mirror experiments to study ring current activity during storm as well as the particle acceleration mechanism in the aurora at solar minimum in occurrence distributions

Our findings are useful to explain electromagnetic ion - cyclotron emissions and perpendicular energisation a

observationally reported by Lund [19] for the auroral acceleration region However, it may be useful to explain other observations wherever, the magnetic mirror type of geometry is considered The effect of loss-cone distribution is to enhance the growth rate of the EMIC wave, as well as to increase the energy of the resonant ions in the presence of wave. The transversely accelerated ions and their association with EMIC waves in the auroral acceleration region have been recently reported by various workers in the analysis of FAST satellite data [36]. The equilibrium dipolar magnetic field of the earth is curved in a meridional plane and introduces the loss-cone effects in the particles distribution function Hence the study of the EMIC wave in auroral acceleration region with steep loss-cone distribution is of importance to explain the observations of the FAST satellite [19] The diffusion of particles into the loss-cone during the recovery phase of the storm is important and may be sidered in further studies.

Acknowledgment

One of authors (PV) is thankful to Department of Science & Technology (DST), New Delhi for financial assistance

References

[1] J M Cornwall, F V Coroniti and R M Thorne *J Geophys Res* **75** 4699 (1970)

[2] J M Cornwall H H Hilton and P F Mizera *J Geophys Res* **76** 5220 (1971b)

[3] J M Cornwall and M Schulz *J Geophys Res* **76** 7791 (1971)

[4] S Cuperman and L Gomberoff *J Plasma Phys* **18** 391 (1977)

[5] V K Jordanova C J Farrugia R M Thorne G V Khazanov, G D Reeves and M F Thomson *J Geophys Res* **106** 7 (2001)

[6] E J Lund E Mobius, K A Lynch, D M Klumpar, W K Peterson, R E Ergun and C W Carlson *Phys Chem Earth* © **26** 161 (2001)

[7] L R Lyons and R M Thorne *J Geophys Res* **77** 5608 (1972)

[8] W D Gonzalez, B T Tsurutani A L C Gonzalez, E J Smith, F Tang and S I Akasofu *J Geophys Res* **94** 8835 (1989)

[9] R M Thorne and R B Horne *J Geophys Res* **102** 14155 (1992)

[10] R M Thorne and R B Horne *J Geophys Res* **99** 17, 275 (1994)

[11] J M Cornwall, F V Coroniti and R M Thorne *J Geophys Res* **76** 4428 (1971a)

[12] R Gendrin and A Roux *J Geophys Res* **85** 4577 (1980)

[13] R M Thorne and R B Horne *Geophys Res Lett* **19 417** (1992)

[14] R M Thorne and R B Horne *J Geophys Res* **102** 11457 (1997)

[15] B J Fraser *Planet Space Sci* **30** 1229 (1982)

[16] A Korth, G Kremser, S Perrault and A Roux *Planet Space Sci* **32** 1393 (1984)

[17] B J Anderson and S A Fuselier *J Geophys Res* **99** 19413 (1994)

[18] R E Erlandson and B J Anderson *J Geophys Res* **101** 7843 (1996)

[19] E J Lund, E Mobius, C W Carlson, R E Ergun, L M Kistler B Klecker D M Klumpar, J P McFadden M A Popecki, R J Strangeway and Y K Tung *J Atmos Terr Phys* **62** 467 (2000)

[20] K A Lynch R L Arnoldy, P M Kintner and J Bonnell *Geophys Res Lett* **23** 3293 (1996)

[21] M Andre, P Norqvist, L Andersson, L Eliasson, A I Eriksson L Blomberg, R E Erlandson and J Waldemark *J Geophys Res* **103** 4199 (1998)

[22] E J Lund, E Mobius, L Tang, L M Kistler, M A Popecki, D M Klumpar, W K Peterson, E G Shelley B Klecker D Hovestadt, M Temerin R E Ergun, J P McFadden, C W Carlson F S Mozer, R C Elphic, R J Strangeway, C A Cattell and R F Pfaff *Geophys Res Lett* **25** 2049 (1998)

[23] R E Erlandson, L J Zanetti, M H Acuna A I Eriksson L Eliasson M H Boehm and L G Blomberg *Geophys Res Lett* **21** 1855 (1994)

[24] A Vaivads, M Andre, P Norqvist T Oscarsson K Ronnmark L Blomberg, J H Clemmons and O Santolik *J Geophys Res* **104** 2563 (1999)

[25] D J Gorney, A Clarke D Croley, J Fennell J Luhmann and P Mizera *J Geophys Res* **86** 83 (1981)

[26] M S Redsum, M Temerin and F S Mozer *J Geophys Res* **90** 9615 (1985)

[27] E J Lund and J LaBelle *J Geophys Res* **102** 17241 (1997)

[28] M Temerin and R L Lysak *J Geophys Res* **89** 2849 (1984)

[29] M S Tiwari and P Varma *Planet Space Sci* **41** 199 (1993)

[30] A K Dwivedi, P Varma and M S Tiwari *Planet Space Sci* **49** 993 (2001)

[31] K D Misra and M S Tiwari *Can J Phys* **57** 1124 (1979)

[32] P Varma and M S Tiwari *Indian J Pure & Appl Phys* **31** 616 (1993)

[33] R Mishra and M S Tiwari *Indian J Pure & Appl Phys* **42** 104 (2004)

[34] M S Tiwari and P Varma *J Plasma Phys* **46** 49 (1991)

[35] P Varma and M S Tiwari *Physica Scr* **45** 275 (1992)

[36] G Ahirwar, P Varma and M S Tiwari *Ann Geophys* **24** 1919 (2006)

[37] C F Kennel and H E Petschek *J Geophys Res* **71** 1 (1967)

[38] D Summers and R M Thorne *J Plasma Phys* **53 293** (1995)

[39] V K Bajaj and M S Tiwari *Indian J Pure & Appl Phys* **30** 198 (1992)

[40] M S Tiwari and G Rostoker *Planet Space Sci* **32** 1497 (1984)

[41] A K Dwivedi, P Varma and M S Tiwari *Planet Space Sci* **50** 93 (2002)

[42] J U Kozyra, T E Cravens, A F Nagy, E G Fontheim and R S B Ong *J Geophys Res* **89** 2217 (1984)

[43] T Chang, G B Crew N Heishkowitz J R Jasperse, J M Retterer and J D Winningham *Geophys Res Lett* **8** 636 (1986)

[44] H L Collin, W K Peterson, J F Drake and A W Yau *J Geophys Res* **93** 7558 (1988)

[45] B J Fraser F W Menk and C L Waters Cooperative research center for satellite system & school of mathematical and physical sciences University of Newcastle NSW 2308 Australia (2004)

[46] E J Lund E Mobius, D M Klumpar, L M Kistler, M A Popecki, B Klecker, R E Ergun, J P McFadden, C W Carlson and R J Strangeway *Adv Space Res* **23** 1721 (1999)